

光学学报

地基 Mie 散射激光雷达反演的研究进展与挑战

毛飞跃^{1,2}, 徐维维¹, 臧琳³, 潘增新^{2,4}, 龚威^{2,3*}

¹武汉大学遥感信息工程学院, 湖北 武汉 430079;

²武汉大学测绘遥感信息工程国家重点实验室, 湖北 武汉 430079;

³武汉大学电子信息学院, 湖北 武汉 430079;

⁴耶路撒冷希伯来大学地球科学研究所, 以色列 耶路撒冷 91904

摘要 云和气溶胶是地球大气系统的重要组成部分,对大气环境、气候变化和人类健康有着重要影响。近几十年来,Mie 散射激光雷达以其全天候、高时空分辨率和垂直分布探测的优势备受关注,在云和气溶胶特性研究及大气环境监测中获得了广泛应用。本文简要介绍了 Mie 散射激光雷达的探测原理和发展历程,重点梳理了 Mie 散射激光雷达中的重叠因子修正、层次检测和信号反演等关键问题的研究进展与挑战,并对相关技术和方法的特点及其适用性进行了探讨,最后对 Mie 散射激光雷达数据反演的未来研究方向进行了展望。

关键词 大气光学; 气溶胶; 重叠因子; 层次检测; 数据反演

中图分类号 P412.25 **文献标志码** A

DOI: 10.3788/AOS222188

1 引言

云和气溶胶是地球大气系统中的重要部分。云和气溶胶具有复杂的物理、化学和光学性质,对大气环境、气候变化和人类生活有着重要的影响^[1]。认识云和气溶胶的各类性质、时空分布以及传播机理,对于气候变化和大气污染的研究和治理具有重要的意义。遥感手段可以观测和反演云和气溶胶的光学厚度、消光系数、单次散射反照率等光学属性,并且可以通过光学属性推导云和气溶胶的类型和粒径分布等物理信息,目前已经获得了广泛的应用。常用的被动传感器,如太阳光度计和辐射计等,主要依赖于太阳光源进行观测,能够在白天获取云和气溶胶柱积分信息。主动传感器采用人工辐射源发射特定的电磁波来探测气溶胶和云粒子,具有不受观测时间和天气影响的探测优势。其中,激光雷达由于工作波长较短,能够与气溶胶或云粒子直接发生作用,具有高单色性和高指向性,可以获取高时空分辨率的大气粒子特性的垂直分布信息,成为探测大气中云和气溶胶的有力工具,并得到了广泛的应用^[2]。

激光雷达根据工作机制的不同可以分为 Mie 散射、Rayleigh 散射、Raman 散射和荧光激光雷达等^[3-6]。当探测的粒子大小接近或大于激光波长所发生的弹性散射现象时称为 Mie 散射,而当粒子远小于激光波长

时,则会发生 Rayleigh 散射。Mie 散射信号较强,探测相对简单,但其存在一个方程求解两个未知数(消光系数和后向散射系数)的病态反演问题,需要假设激光雷达比(消光系数与后向散射系数之比),引入了一定的不确定性。此外,高光谱分辨率激光雷达技术能够实现 Mie 散射和 Rayleigh 散射信号分离,可以避免 Mie 散射激光雷达的病态反演问题^[7-13]。但高光谱分辨率激光雷达目前存在系统结构复杂、技术难度大和价格昂贵等问题,而且在求解消光系数时存在信号求导过程,导致反演结果不确定性仍然较大,需要进一步的降噪处理,限制了高光谱分辨率激光雷达的推广应用。总体上,由于 Mie 散射激光雷达具有回波信号较强、系统结构简单和易于实现的特点,目前仍是应用最为广泛的云和气溶胶探测激光雷达^[14-15]。

Mie 散射激光雷达已经具有较长的发展历史,1963 年,Fiocco 等^[16]首次使用红宝石 Mie 散射激光雷达接收到了 60~140 km 高层大气的微弱回波信号。1966 年,中国科学院大气物理研究所成功研制了我国第一台红宝石 Mie 散射激光雷达^[17]。之后很多国内学者都开始了 Mie 散射激光雷达的研制,波长主要是 532 nm 或 1064 nm,对区域对流层和平流层气溶胶光学特性进行了观测和分析^[18-20]。在 20 世纪 70 年代, Schotland 等^[21-23]开始将偏振激光雷达用于云和平流层气溶胶偏振特性的测量,其主要通过使用偏振分束器

收稿日期: 2022-12-30; 修回日期: 2023-02-19; 录用日期: 2023-04-21; 网络首发日期: 2023-05-08

基金项目: 国家自然科学基金(41971285,42201344)

通信作者: *weigongwhu@163.com

后将后向散射光分成平行分量和垂直分量回波信号,可以获取粒子的退偏比属性。由于非球形粒子(如沙尘和卷云冰晶等)的后向散射光会存在退偏现象,因此偏振激光雷达对于探测非球形粒子具有独特的优势,退偏比也常用于区分冰云和水云以及识别沙尘、烟尘等气溶胶。1989年,Sasano等^[24]首先使用多波长散射激光雷达探索气溶胶类型分类和后向散射系数反演。1991年,中国科学院安徽光学精密机械研究所成功研制了多波长激光雷达系统,之后国内其他单位也先后研制了多种双波长(532 nm和1064 nm)和三波长(355、532、1064 nm)的Mie散射激光雷达^[25-32]。相比单波长激光雷达,多波长激光雷达除了能获取更多波段的颗粒散射信息,还可以外推颗粒尺寸分布等微物理特性。近年来,国内开展了大量的多波长偏振Mie散射激光雷达研制和观测应用,可以对云和气溶胶的物理光学特性进行更精细的探测,并且由于其具有结构简单、成本低廉的特点,在目前激光雷达系统中几乎都配置了多波长和偏振的观测通道^[33-35]。

为研究区域和全球的大气成分时空演变,国内外相继发展出了各种地基激光雷达网络,如美国的微脉冲激光雷达网(MPLNET)^[36]、欧洲气溶胶研究激光雷达网(EARLINET)^[37]、欧美联合组建的大气成分变化探测网(NDACC)^[38]、亚洲沙尘激光雷达网(ADNET)^[39]、“一带一路”激光雷达网^[6]、拉丁美洲激光雷达网(LALINET)^[40]、美国东部激光雷达观测网(REALM)^[41]和苏联组建的激光雷达网(CIS-LINet)^[42]等。其中大部分以Mie散射激光雷达为主,通过联网可以实现大范围的大气垂直分布信息的协同探测。除固定站点的地基激光雷达系统之外,国内外研究学者相继发展了结构紧凑、质量较轻、便于携带和移动的小型Mie散射激光雷达,通过车载和船载等平台走航观测,可以有效丰富区域大气环境的监测资料^[43-45]。这些地基网络以及本地站点和移动式Mie散射激光雷达,在全球和区域的气溶胶和云监测中发挥了重要的作用。

随着工业化的发展,Mie散射激光雷达的硬件变得成熟和普遍,使得人们对数据反演和分析的需求越来越迫切。然而,现在Mie散射激光雷达数据处理还存在一些难点,导致反演结果的不确定性较大,难以发挥其大气探测潜力。地基Mie激光雷达的一个重要目标是反演垂直廓线的大气光学参数信息,并且通过垂直积分可以进一步获得气溶胶光学厚度等参数。然而由于几何重叠因子产生的低空观测信息缺失,而近地表的大气信息往往最受人们关注,因此校正重叠因子是激光雷达数据处理中的一个关键问题。此外,识别和提取激光雷达信号中的云和气溶胶层次的分布信息,是后续光学参数反演和大气研究中的重要需求。为获得最终的光学参数信息,信号反演是激光雷达数据处理中的核心步骤,也是相关研究中关注的重点。

针对上述问题,本文在简单介绍地基Mie散射激光雷达探测原理的基础上,主要总结了目前地基Mie散射激光雷达中的重叠因子修正、层次检测和信号反演的研究进展,对当前相关方法的适用性进行了深入分析,有助于未来Mie散射激光雷达的研究和应用。

2 地基Mie散射激光雷达原理

考虑双成分单次散射的单波长弹性激光雷达方程的功率表达式^[46]为

$$P(r) = \frac{C}{r^2} \cdot P_0 \cdot G(r) \cdot \beta(r) \cdot \exp \left[-2 \int_0^r \alpha(r) dr \right] + e(r), \quad (1)$$

式中: $P(r)$ 代表接收高度 r 处的信号; C 为激光雷达常量,与激光雷达的配置有关; P_0 代表激光初始发射能量; G 为重叠因子,即接收的能量与到达望远镜反射镜的能量之比; β 为大气后向散射系数,是粒子和大气分子的后向散射系数 β_p 和 β_m 之和; α 为大气消光系数,是粒子和大气分子的消光系数 α_p 和 α_m 之和; $e(r)$ 为噪声,一般可认为是高斯噪声。

理想大气条件下的模拟信号如图1(b)中的虚线所示,而实际中的观测信号往往如图1(b)中的实线所示。因为激光束和信号接收望远镜的光轴并不重合,实际中的观测在近地面只能接收到部分信号,对这些信号直接进行反演将会有很大的误差,所以需要预先对信号进行重叠因子修正以归一到信号全部接收的状态。此外,如图1(c)中三角形标记的突起层次信号所示,探测云和气溶胶层次的悬浮位置及其类型也是大气激光雷达数据处理的重要任务之一。进一步地,在地基Mie散射激光雷达的后向散射和消光反演算法方面,目前标准算法仍然受到边界值选择、激光雷达比(消光系数与后向散射系数比)的确定和噪声干扰等因素的影响。因此重叠因子的影响、云和气溶胶层次检测的困难和激光雷达方程的病态性,是当前激光雷达数据处理中的主要不确定性来源和待解决的关键问题。

3 重叠因子修正

在激光雷达探测大气的过程中,由于激光发射器和接收器之间硬件结构(如望远镜接收角、激光发散角、激光束与望远镜两者中心间距等)的影响,在一定的范围内只有一部分后向散射光被望远镜接收,被望远镜接收的能量与该距离上后向散射总能量之比称为该距离上的重叠因子^[47]。激光雷达系统重叠因子的典型几何示意图如图2所示,其中 d_{T0} 代表接收望远镜的有效直径, d_{L0} 为激光束的初始直径, θ 为发射角, α 为接收器的接收角, $d0$ 为两轴间的距离, ω 为发射器与接收器的倾斜度。当激光脉冲横穿整个透射距离 r 时,距离 d 可近似表示为 $d0 - r \cdot \omega$ 。激光束半径和接收望远镜的接收半径为

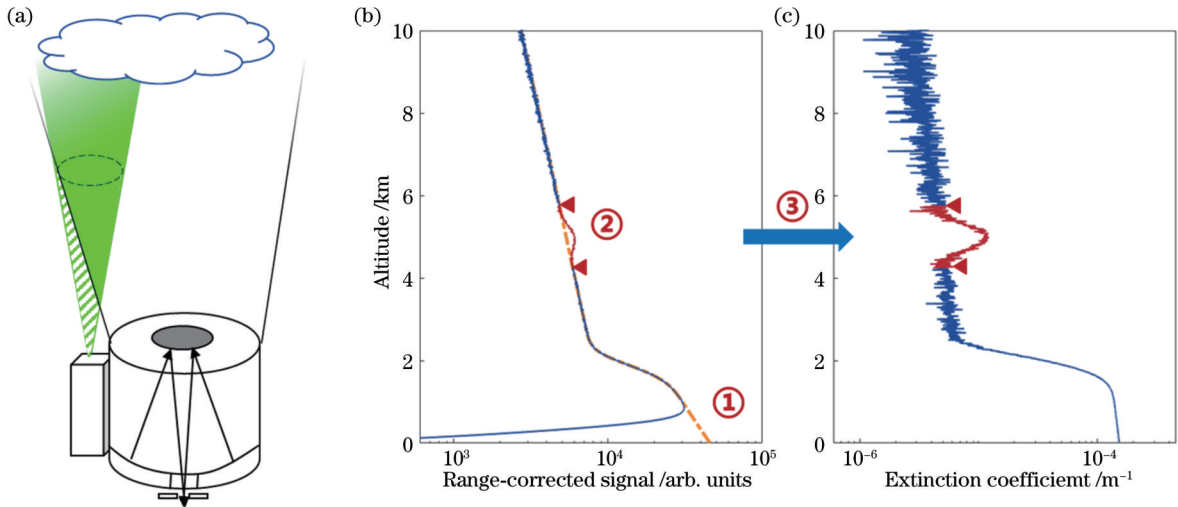


图 1 激光雷达探测和数据处理存在的问题:①重叠因子修正;②云和气溶胶层次检测;③数据反演。(a)激光雷达探测原理图;(b)虚线为洁净大气的信号,而实际的观测信号往往如图中的实线所示(其中三角形标记之间的范围为层次,其余为均匀大气);(c)由观测信号反演的消光系数

Fig. 1 Issues in lidar detection and data processing: ① overlap factor correction; ② cloud and aerosol layer detection; ③ data retrieval. (a) Schematic diagram of lidar detection; (b) dashed line is clear atmosphere signal, while actually observed signal is usually shown as solid line (range between triangle marks is layer and rest represents uniform atmosphere); (c) extinction coefficients retrieved from observed signal

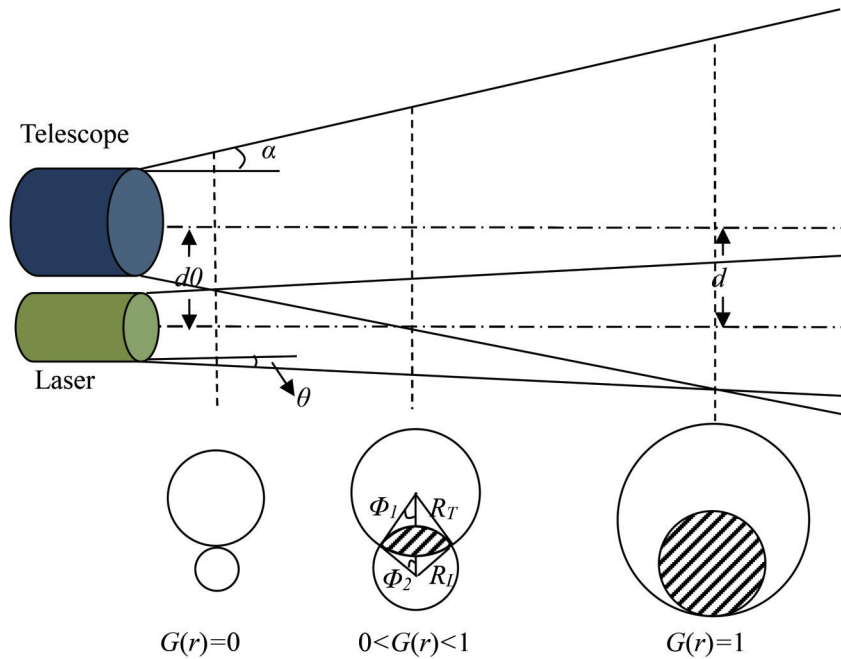


图 2 激光雷达观测的几何结构随距离 r 的变化情况^[48]

Fig. 2 Geometric structure of lidar observation varies with distance r ^[48]

$$\begin{cases} R_L = \theta \cdot r + \frac{d_{L0}}{2} \\ R_T = \alpha \cdot r + \frac{d_{T0}}{2} \end{cases} \quad (2)$$

为了将低空区域的大气回波信号归一到全部接收状态,相关学者提出了多种求解重叠因子的方法,大致可以分为实验法^[49-51]和理论法^[47, 52-58]两类。传统实验法一般选择天气晴朗、污染少的夜晚,通过将激光雷达

水平放置测量,在大气水平分布均匀的假设下,对测量信号进行拟合外推得到近场的重叠因子。实验法不需要了解激光雷达的系统参数,通过实际测量的激光雷达信号可以计算得到较为精确的重叠因子结果。通过联合星载激光雷达和地面激光雷达信号,也可以获得地面激光雷达的重叠因子,然而星地激光雷达的视场很难完全匹配^[50]。此外,有些实验法如重叠因子的迭代算法,能够很好地应用于特定的激光雷达如 Raman

激光雷达,但这些方法对仪器的配置有一定的要求^[59-61]。总体上,实验法测量较为精确,但是一次只能获得一个状态下的实验数据,很难应用于激光雷达信号的实时模拟和指导激光雷达光学系统配置的实时优化^[47]。

理论法可以分为解析法^[47, 52-54]和光线追踪法^[55-56]。虽然传统解析法简单实用,但是它们需要假设激光束是理想的均匀或者高斯分布,还需要假设接收概率因子恒为 1,因此带来很大的误差^[55]。特别是当实际激光束能量分布与理想分布相差甚远的时候,会带来不可忽视的误差,并且激光雷达系统的激光强度分布、激光束指向和角度参数也往往难以精确地获取。光线追踪法可以克服解析法理论上的不足,能够考虑任意的激光能量分布,是理想的激光雷达系统建模方式。但是光线追踪法需要考虑数值孔径、探测器模型、衍射效应、望远镜视场权重和机械结构遮挡等多种因素,其校正可靠性依赖于复杂的模型构建^[11, 55-56]。此外, Gong 等^[48, 62-63]提出了基于激光强度分布和基于蒙特卡罗积

分的重叠因子计算方法,基于激光强度分布的方法同时具有解析法与光线追踪法的优点,可应用于指定激光强度分布的计算。

理论法的一个主要优势是可以指导激光雷达的设计,而激光雷达系统本身的硬件设计也会影响重叠因子,例如重叠因子与激光发射角和望远镜接收半角的关系如图 3 所示。从图 3 (a)中可以看出,在其他参数设置为默认值的情况下,激光发射角越小(大),进入望远镜视场的距离越大(小),重叠因子达到 1 的高度越低(高)。然而当激光发射角大于望远镜接收半角时[如图 3 (a)中的 0.7 mrad 虚线所示],远场的重叠因子不能达到 1。在图 3 (b)中,越大的望远镜接收半角越有利于激光进入望远镜接收视场,而且重叠因子上升也会更快。上述结果表明,激光发射角越小,望远镜接收角越大,越有利于低空大气的探测。但实际情况中,望远镜的接收半角越大,会引入更多的背景噪声,有效探测高度也会比较低,因此需要小的望远镜接收半角来抑制背景噪声。

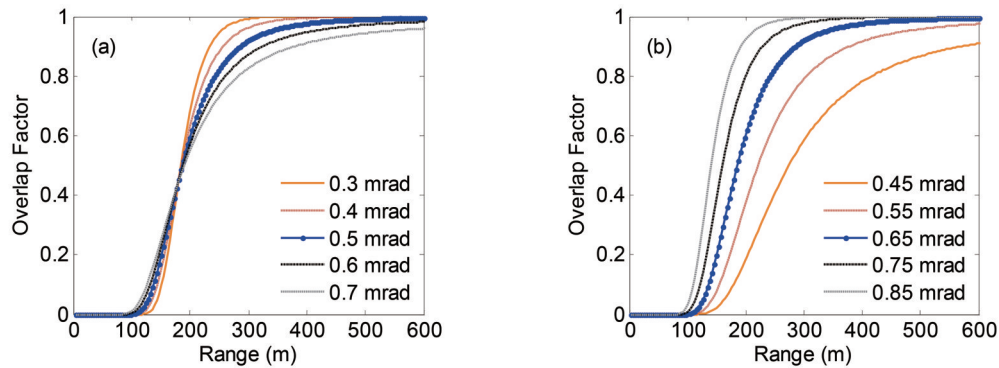


图 3 重叠因子随激光发射角 θ 和望远镜接收半角 α 的变化^[48]。(a)重叠因子随 θ 的变化;(b)重叠因子随 α 的变化

Fig. 3 Overlap factor varies with laser emission angle θ and telescope receiver half angle α ^[48]. (a) Overlap factor varies with θ ; (b) overlap factor varies with α

除了上述信号修正的方式减少重叠因子的影响,还可以通过激光雷达硬件的改进直接减少重叠因子的影响。例如可以通过采用两个望远镜系统分别接收高低空信号的双视场激光雷达技术,有效减小重叠因子的影响范围,实现低盲区的近场探测^[64-66],但同时激光雷达主副视场观测的大气范围不同,在信号强度和特征上会存在一定的差异^[67]。此外,CCD 侧向散射激光雷达通过将 CCD 相机放置在一定距离上观测激光束,理论上可以实现无盲区的探测,适合在夜间探测近距离的粒子后向散射^[68]。CCD 侧向散射激光雷达假设在探测范围内气溶胶的相函数是均匀的,通常将地面观测的气溶胶相函数使用到各个高度上进行反演^[69]。当然,气溶胶相函数是由粒径分布和折射率等因素所决定,均匀假设难免会引入一定的不确定性,所以通常需要进行修正。总体上,目前新型的双视场和 CCD 侧向散射激光雷达在低空重叠因子影响区域具有观测优势。

目前重叠因子的校正方法可大致分为实验法和理

论法。实验法不需要了解激光雷达系统参数,但是要求大气水平分布严格满足均匀条件,现实中难以做到,并且难以用于指导激光雷达设计。而理论法可分为解析法和光线追踪法,能够辅助指导激光雷达的设计安装。此外,通过激光雷达硬件和相应软件的改进,如双视场和 CCD 侧向散射等激光雷达,能够更加有效地减小重叠因子的影响。

4 云和气溶胶层次检测

云与气溶胶层次检测是激光雷达数据处理的最重要步骤之一,如何在 Mie 散射激光雷达数据中自动地检测出这些大气层次,是一个历经多年的难题^[70-71]。层次检测的本质是从激光雷达的背景信号和噪声中提取云和气溶胶层次的边界位置。2005 年, Kovalev 等^[72]指出,层次的边界可以容易地根据信号时空变化由人眼进行识别,但是很难精确地自动判定。针对该问题,目前发展了较多的激光雷达层次检测算法,主要

包括基于信号强度相对变化的方法、基于阈值的方法和基于统计的方法等。此外,深度学习的技术在层次检测中也有应用,但目前缺乏可靠的训练样本,因此其应用案例仍相对较少^[73]。

基于信号强度相对变化的方法是利用激光雷达信号遇到层次会出现强度增强的特点,通过识别信号的这些变化来确定层次,可以直接应用于未定标的原始信号。基于信号强度的方法包括了斜率法、小波法和趋势函数法等。斜率法利用信号的一阶导数(斜率)的过零位置来确定层次边界^[70],但是如图 4 (b)所示,当激光雷达信号受到噪声严重干扰时,信号求导得到的斜率会反复过零,导致这种方法近乎失效。小波法具有很好的抗噪性,主要通过寻找激光雷达信号的局部极值点来识别层次。但层次边缘附近的信号变化缓慢,并不足以产生局部模极大值,因此层次边界的定位存在较大偏差^[74]。Mao 等^[75]提出了一种基于趋势函数的简单多尺度算法用于地基激光雷达层次检测,相比于斜率法和小波法能够更好地捕捉到层次信号的变化。陈思颖等^[76]进一步提出了一种改进的简单多尺度法,通过引入尺度个数阈值作为检测判据,提升了云底高度检测的准确性。但是,对于信噪比极低的高空区域,简单多尺度算法仍然具有改进空间。

基于阈值的方法是通过识别信号值是否连续超过

阈值序列来判定层次,阈值序列由理想信号加上一定的不确定性范围获得,相比于斜率法更为稳健,目前在地基和星载激光雷达的云和气溶胶产品生产中被广泛使用^[77]。Vaughan 等^[78]提出了一种选择性迭代边界定位(SIBYL)算法检测云和气溶胶层次,目前作为官方算法应用于 CALIPSO 星载激光雷达。SIBYL 算法通过一种自适应的阈值序列进行层次探测,每检测出一个特征层次,即会对下方的检测阈值序列进行衰减校正的调整,以此适应这种层次造成的信号衰减并避免下方弱层次的漏检。但许多研究表明,这种阈值法仍然会漏检大量的光学薄层,尤其是在白天信噪比较低的情况下^[79-80]。由于阈值法主要是对校正后的激光雷达信号进行检测,因此主要应用于具有高空清洁大气探测与校正的星载激光雷达。Lewis 等^[81]在 MPLNET 地基激光雷达产品中使用了一种斜率法和阈值法相结合的云层检测算法,通过斜率法对低空大气进行检测,并识别一段清洁大气作为归一化区域,在归一化区域以上再使用阈值法检测层次。这种组合的方法相比之前版本的产品检测性能有了较大提升,但阈值法仍然存在不足。图 4 (c)展示了阈值法在地基激光雷达中的应用,阈值法对于 8~10 km 左右的强层次能够很好地识别,但 7 km 左右的微弱层次由于难以连续超越阈值而会被漏检。

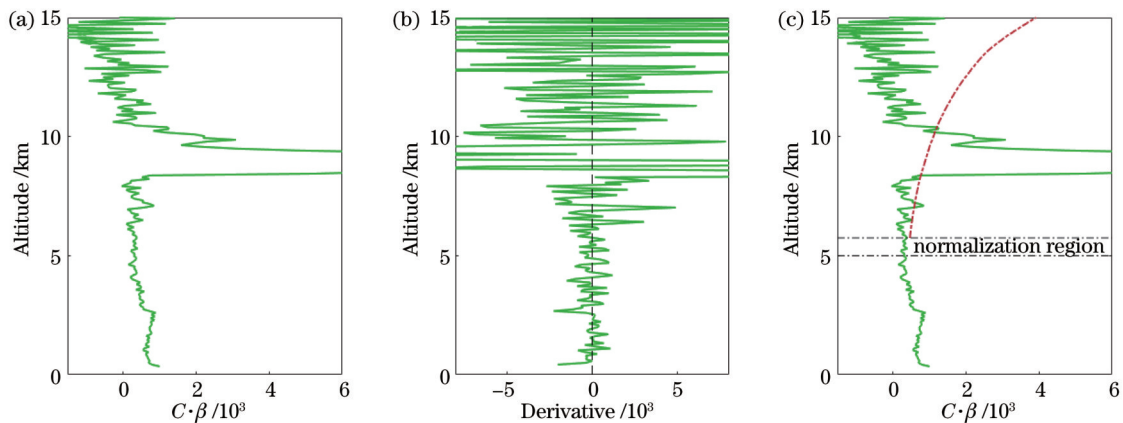


图 4 斜率法和阈值法的检测示意图。(a)地基激光雷达观测信号;(b)地基激光雷达信号的斜率;(c)地基激光雷达的层次检测阈值(虚线)

Fig. 4 Schematic diagram of detection by slope method and threshold method. (a) Ground-based lidar observation signal; (b) slope of ground-based lidar signal; (c) layer detection threshold of ground-based lidar (dashed line)

近期,Mao 等^[83]提出了一种基于伯努利分布假设的多尺度算法,成功应用于 CALIPSO 层次检测,该算法避免了阈值和斜率的限制,检测性能优于 CALIPSO 官方产品。该方法尝试将层次检测转化为数理统计上的伯努利分布假设检验问题,通过设置一定的置信度(例如 0.01)判断信号的变化是否属于层次,使其较好摆脱之前对经验参数的依赖。Xu^[82]通过联合基于趋势函数和伯努利分布的多尺度层次检测算法,发展了一种适用于地基激光雷达的云检测算法。

同时,为了从检测层次中提取出云层,参考了 MPLNET 官方算法使用斜率阈值、信号标准差阈值和光学厚度阈值分类出云层^[81]。联合多尺度云层检测算法的结果如图 5 所示,相比于 MPLNET 官方算法能够更好地检测薄云层次和定位层次的边界。与基于信号强度和阈值的检测方法相比,该多尺度检测方法对弱层次检测具有显著优势。

在目前的激光雷达层次检测方法中,基于信号强度变化的方法能够直接应用于原始的激光雷达信号,

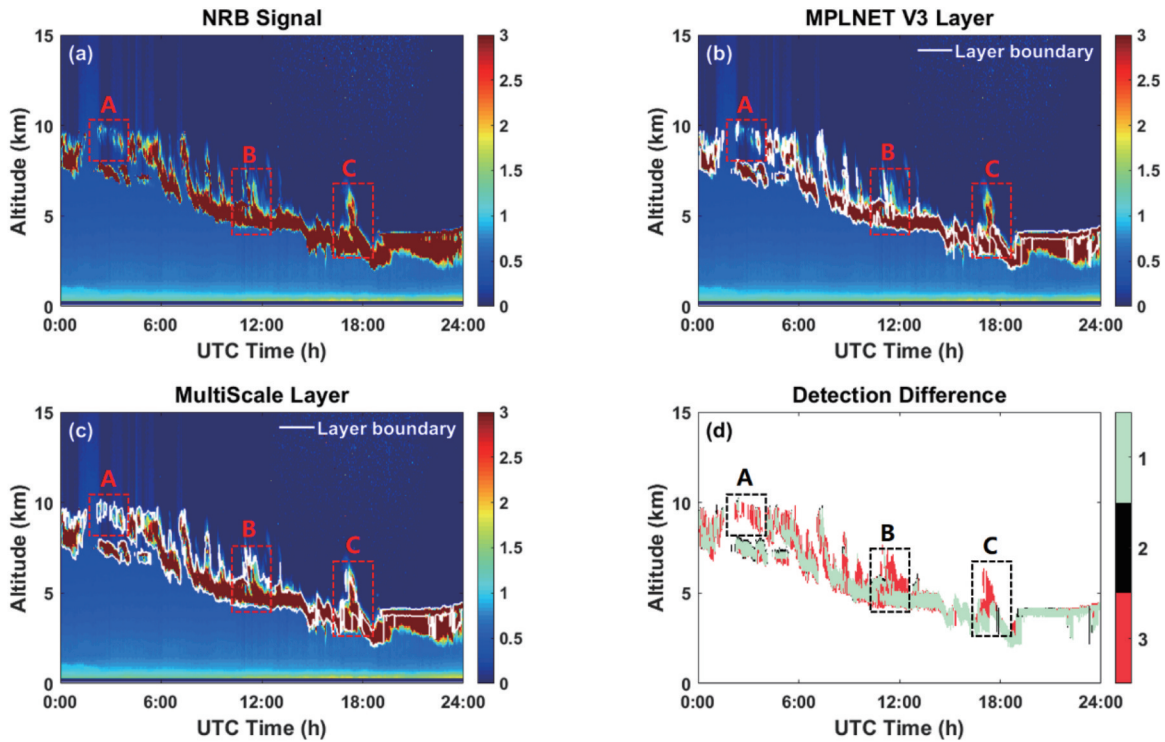


图 5 联合多尺度算法和 MPLNET 产品的场景检测对比^[82]。(a)地基激光雷达回波信号;(b) MPLNET 产品的云层检测结果;(c)联合多尺度算法的云层检测结果;(d)两种方法的云层检测差异,其中标签“1”、“2”和“3”分别代表两种算法共有的检测、MPLNET 产品独有的检测和联合多尺度算法独有的检测

Fig. 5 Comparison of joint multiscale algorithm and MPLNET product for scene detection^[82]. (a) Ground-based lidar echo signal; (b) cloud layer detection results for MPLNET product; (c) cloud layer detection results for joint multiscale algorithm; (d) differences in cloud detection between two methods, where label "1", label "2", and label "3" represent common detections of both methods, unique detections of MPLNET product, and unique detections of joint multiscale algorithm, respectively

但同时受信号噪声影响也最大。基于阈值的方法相比于基于信号强度的方法更为稳健,在相关的激光雷达产品生产中被广泛使用,但弱信号引起信号波动难以持续超越阈值,因而存在光学薄层漏检的问题。基于伯努利分布假设检验的方法从数理统计的角度提供了一种估算信号属于特征层次的方法,在相关研究中表明其检测性能要优于基于阈值的方法,在未来的激光雷达层次检测中具有较大的应用和发展潜力。

5 激光雷达信号反演

自 20 世纪 60 年代起,基于激光雷达探测反演大气

参数的方法论被陆续建立^[84-88]。Collis 基于均匀大气分布的假设前提,提出将一种斜率法用于大气消光系数的反演^[89]。Collis 斜率法虽然简便,但由于实际情况中很难存在均匀的大气分布,因此在信号反演中并不常用,但可以用于边界值确定。之后 Klett^[85]和 Fernald^[86]分别利用单成分和双成分大气模型,提出了稳定的反演方法,获得了广泛的应用。Klett 法只考虑了单成分,可以用于当气溶胶散射明显大于分子散射情况下的反演。Fernald 法对气溶胶和分子成分进行分别对待,适用范围比 Klett 法更加广泛,因此反演中使用较多是 Fernald 法。Fernald 法包含后向与前向两部分,表达式分别如下^[46, 85-86]:

后向为

$$\beta_p(i-1) = \frac{X(i-1)\exp[A(i-1)]}{\frac{X(i)}{\beta(i)} + S_p\{X(i) + X(i-1)\exp[A(i-1)]\}\Delta r} - \beta_m(i-1), \quad (3)$$

前向为

$$\beta_p(i+1) = \frac{X(i+1)\exp[-A(i)]}{\frac{X(i)}{\beta(i)} - S_p\{X(i) + X(i+1)\exp[-A(i)]\}\Delta r} - \beta_m(i+1), \quad (4)$$

式中： $A(i)$ 为 $[S_p(i) - S_m(i)][\beta_p(i) + \beta_m(i+1)]\Delta r$ ； $\beta_p(i)$ 为粒子后向散射系数； $\beta_m(i)$ 为分子后向散射系数； $S_p(i) = \alpha_p(i)/\beta_p(i)$ 为粒子的激光雷达比； $S_m(i) = \alpha_m(i)/\beta_m(i) = 8\pi/3$ 为分子的激光雷达比。

Fernald 法方程中还需要给定气溶胶的激光雷达比和边界值(即用于标定的气溶胶后向散射系数)这两个参数才能进行反演,同时通常需要对激光雷达信号进行去噪处理。而且在不同人员使用 Fernald 法的情况下,其假设的边界值和激光雷达比,以及使用的去噪方法通常存在差异^[90],导致反演结果存在一些差异。

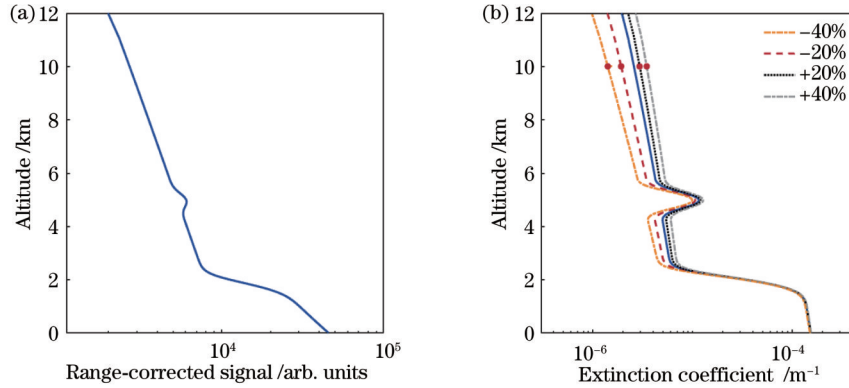


图 6 边界值选择对激光雷达反演的影响。(a)地基激光雷达的模拟信号;(b)消光系数的真值(实线)和反演值(其他曲线)。其中点代表反演选择的边界值,从左至右的曲线(实线除外)表示边界值偏差分别为-40%、-20%、+20%和+40%的反演结果

Fig. 6 Influence of boundary value selection on lidar retrieval. (a) Simulated signal of ground-based lidar; (b) true value (solid line) and retrieval value (other lines) of extinction coefficients. Dots represent boundary values selected for retrieval, and lines from left to right (excluding solid line) indicate retrieval results with boundary value deviations of -40%, -20%, +20%, and +40%, respectively

一般来说,在激光雷达能够探测到对流层顶的情况下,可以在对流层顶选择标定高度,通常认为对流层顶处的后向散射系数主要为大气分子的贡献,这时的边界值选择固定的经验后向散射比。固定后向散射比法通过假设一个特定值的后向散射比来确定边界值,根据前期一个大气背景周期内的观察,标定高度一般选择 10 km 以上,报道的作为边界值的气溶胶后向散射比包括 1.01、1.02 和 1.05 等^[91]。此外,通过分析长期的星载激光雷达背景大气观测,可以获得全球不同地区的经验后向散射比用于地基激光雷达反演^[92]。

当激光雷达受仪器本身或云影响时,探测高度会低于对流层顶高度。而低层大气的气溶胶类型和浓度时空变化复杂,后向散射比不能简单假设为某一固定值。为此研究人员发展了多种拟合方法用于估计边界值,按是否区分气溶胶和大气分子的贡献,可以将这些方法分为单成分拟合法和双成分拟合法。斜率法是一种经典的单成分拟合法,假设大气均匀分布的情况下,通过拟合斜率得到消光系数作为边界值,但在实际大气中这种简单假设会引入一定的误差^[93-96],之后研究人员发展了最小二乘等拟合优化方法^[97-98]。此外,根据 Klett 单成分方法的假设,低空探测时气溶胶的后

5.1 边界值选择

在激光雷达反演中,边界值作为反演初值其存在的误差会直接影响反演结果的精度。图 6 中通过激光雷达信号进行模拟仿真,其中标定高度选择在 10 km 左右。可以看出,当边界值选择存在正向或负向偏差时,反演的消光系数在 2 km 以上的高度也呈现出了同向偏差,并随着边界值相对误差的增大而增大。为此国内外研究人员发展了多种 Mie 激光雷达反演边界值的选择方法,大致可以分为固定散射比法、单成分拟合法、双成分拟合法和联合观测法等。

向散射贡献要远大于大气分子,并设定后向散射系数和消光系数之间存在乘幂关系,在此理论上使用不动点原理、改进牛顿法等进行边界值的计算^[99-102]。上述单成分方法在气溶胶浓度较低时,反演的消光系数会存在较大误差。

Fernald 方法的思想是将分子和气溶胶两个成分分别处理,特别是在高空反演时是非常必要的,因此研究人员在该思想的基础上发展出了用于确定边界值的双成分拟合法。Ma 等^[103]提出了一种基于迭代求解的双成分拟合法,在推导关于气溶胶消光系数边界值的方程中考虑了大气分子的贡献,模拟结果表明,该方法反演结果具有良好的一致性。Tao 等^[104]在选择清洁大气区域,假定气溶胶和大气分子的后向散射比为常数拟合获取边界值,该方法在低气溶胶下准确性明显优于单成分拟合法,但直接受区域选择质量的影响。为此,Mao 等^[105]提出了一种自动分割的双成分拟合法,通过分割算法自动选取最优区域进行边界值拟合,获得了较高的精度。此外,联合观测法通过联合毫米波雷达等其他观测仪器,约束求解边界值的后向散射系数,也能有效改善反演精度,但同时也对观测仪器配置提出了更高的要求^[106]。

总的来说,边界值选择的方法包括固定散射比法、单成分拟合法、双成分拟合法和联合观测法等。在激光雷达能够探测到对流层顶的情况下,固定散射比法较为实用。在激光雷达探测高度达不到对流层顶时,可以通过假设大气分布均匀或者服从一定的变化规律,拟合得到边界值。其中单成分拟合法往往不单独区分大气分子的贡献,因此在低气溶胶浓度下存在较大误差,而双成分拟合法相比于单成分方法适用性更强,反演精度也更高。同时由于气溶胶波动通常较大,因此自动选择理想的拟合区域非常重要。此外联合观测法可以改进边界值拟合的结果,但是对观测仪器配置提出了更高的要求。

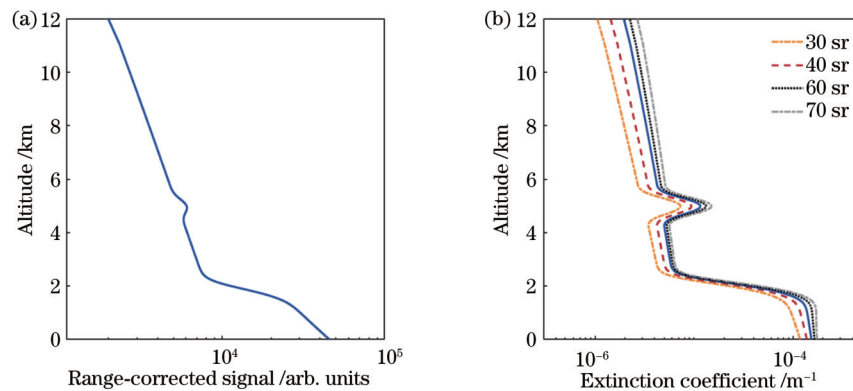


图 7 激光雷达比选择对激光雷达反演的影响。(a)地基激光雷达观测的模拟信号;(b)消光系数的真值(实线)和反演值(其他曲线)。从左至右的曲线(实线除外)表示激光雷达比分别为 30、40、60、70 sr 的反演结果

Fig. 7 Influence of lidar ratio selection on lidar retrieval. (a) Simulated signals of ground-based lidar observation; (b) true value (solid line) and retrieval value (other lines) of extinction coefficients. Lines from left to right (excluding solid line) indicate retrieval results for lidar ratios of 30, 40, 60, and 70 sr, respectively

由于气溶胶存在区域和季节的特征分布,通过长期观测资料可以获得到不同地区的气溶胶类型和其他信息来选择经验的激光雷达比^[108-109]。在 532 nm 的探测波长下,海洋型气溶胶、沙尘型气溶胶和大陆型气溶胶统计的激光雷达比一般为 (23 ± 5) sr、 (44 ± 9) sr 和 (53 ± 24) sr^[110]。然而,气溶胶的时空变异性较大并且常常是多种气溶胶相混合,使用固定的经验值会造成误差的引入。AOD 约束法是目前应用中最为流行的方法,通常使用其他被动辅助仪器(如太阳光度计和 MODIS)观测的 AOD 作为约束,通过迭代不同的激光雷达比反演激光雷达的 AOD,获取与被动观测 AOD 最匹配的解算结果^[111-112]。除 AOD 参数外,地面仪器还可以提供粒子尺寸分布谱、复折射率、相对湿度、氧化污染物等参数用于激光雷达比的反演和分析^[113-115]。然而 AOD 约束法利用的是整层大气的柱积分信息,并且只能在白天和无云层遮挡的条件下进行观测,AOD 约束法仍然存在的限制。同时激光雷达比会随着高度而变化,若整个层次的激光雷达比迭代设置为同一值,会给反演的消光系数引入不确定性。此外,地基激光雷达通常存在探测盲区,如何考虑探测盲区的

5.2 激光雷达比确定

一个激光雷达方程有气溶胶消光系数与后向散射系数两个未知数,这是数据反演的一个难题。现在流行的做法是假设两种系数之间存在一定的比值关系,即激光雷达比,它是气溶胶物化性质的函数^[107]。图 7 模拟了激光雷达比选择对于反演结果的影响,其中真实的激光雷达比为 50 sr,而实际反演中分别选择了 30、40、60、70 sr 用于反演,可以看到,选择偏大或偏小的激光雷达比均会导致反演的消光系数出现整体偏差。目前研究中确定激光雷达比的方法主要可以分为经验激光雷达比法、气溶胶光学厚度(AOD)约束法和联合观测法等。

AOD 贡献也是一个问题。

通过联合不同的廓线观测也可以反演激光雷达比。星地激光雷达之间的联合可以增加解算的激光雷达方程条件,不需要假设激光雷达比就可以直接反演得到气溶胶的消光系数和后向散射系数^[116]。Mao^[92]利用国际空间站平流层气溶胶和气体实验 III (SAGE III)的廓线观测作为约束条件,反演了 CALIPSO 未探测到的微弱气溶胶,并给出了全球平流层和对流层的微弱气溶胶激光雷达比的参考值分别为 42.2 sr 和 24.5 sr,未来该方法也可以推广到地基激光雷达。随着双波长雷达的发展,可以将不同波长之间的后向散射系数曲线相似性作为反演中的额外约束条件,估算气溶胶层的激光雷达比的均值^[24]。但实际气溶胶层内的组成和粒径分布存在着较大变化,这种不同波长的后向散射系数比值恒定的假设也可能会引入误差^[117]。此外,Raman 激光雷达和高光谱分辨率激光雷达等能够独立反演消光系数和激光雷达比等参数,通过联合观测廓线或统计长期的激光雷达比可以辅助 Mie 散射激光雷达的反演^[12, 118]。

如上所述,确定激光雷达比的方法主要有经验激

光雷达比法、AOD 约束法和联合观测法等。经验激光雷达比法使用的是固定激光雷达比,难以满足实时变化的复杂大气监测需求。AOD 约束法通过限制条件可以获得较为准确的整层激光雷达比均值,但缺乏激光雷达比的垂直分布信息。与之相比,联合观测法通过联合 SAGE、Raman 激光雷达等仪器观测,可以获得激光雷达比的垂直分布廓线,但同时也对仪器和观测条件有着特殊要求,因此如何获取高精度的激光雷达比廓线是未来的一个重要研究内容。

5.3 抗噪算法

由于激光雷达信号衰减服从距离平方反比定律,即信号信噪比随着距离平方衰减,这严重影响了数据反演精度以及激光雷达的有效测量距离。此外,白天的强背景太阳光噪声、暗电流噪声和热噪声都会干扰激光雷达的回波信号。激光雷达信号去噪的难点在于保证对噪声敏感的同时,又要避免对信号曲线过于平滑,造成气溶胶观测信息的丢失。为了增强信噪比和有效测量距离,对多次观测数据进行平均是有效的处理方式。理论上将信号噪声降低一半需要平均 4 次观测,若要将噪声进行 n 次减半需要 4^n 次平均,会极大地降低时空分辨率。因此,研究人员发展了多种激光雷达信号去噪方法,如滑动平均法、频率分解法、同化滤波法、联合抗噪法和神经网络法等^[3, 119-121]。

激光雷达信号是非线性不平稳的信号(随距离平方衰减),因此移动平均模型不适合处理此类信号^[3, 120]。频率分解法主要通过频率特征对信号进行分解降噪,主要包括了傅里叶法、小波法和经验模态分解法等。傅里叶法通过傅里叶变化提取信号的频率信息,根据有用信号的频率低于噪声的原则剔除高频的噪声,但对不平稳的激光雷达信号去噪不佳^[122]。小波法则是通过多尺度分析将信号分解为不同的频率项,能有效地提取信号的细节,但存在如何选择合适的小波基函数和分解级别的问题^[123]。另一种经验模态分解法将信号按高频到低频分解成一系列的固有模态函数和残差,不需要任何先验信息,是一种在非平稳非线性信号上广泛使用的方法^[124]。在激光雷达信号的去噪应用中显示,经验模态分解法的性能要优于低通滤波、多脉冲平均方法以及小波法^[124-125]。但经验模态分解的一个重要缺陷是经常出现模态混叠,使得一个固有模式函数中会包含多个时间尺度特征,缺乏明确的物理含义。为此,研究人员提出了集合经验模态分解和变分模态分解等改进方法。集合经验模态分解方法通过在信号中加入小幅度的白噪声,有效抑制原始模型中的模态混叠^[126],而变分模态分解方法是一种自适应和非递归分解算法,可以克服模态混叠问题实现固有模态函数的有效分离^[127]。

Mao 等^[121, 128]提出了考虑激光雷达物理方程约束的抗噪反演算法,该方法将激光雷达方程转换为状态空间模型,垂直信号作为时间序列观测,基于集合卡尔

曼滤波、粒子滤波数据同化滤波器进行消光系数反演,实现了云和气溶胶消光系数的高精度、高时空分辨率反演。Zeng 等^[129]通过机器学习的高斯过程方法改善了集合卡尔曼同化滤波器中的不良预测,有效提升了激光雷达反演方法的去噪和反演精度。在集合卡尔曼滤波迭代过程中,前面的信号点可以为后面的信号点提供反馈用以改善迭代结果,但前面的信号点仍然缺乏反馈信息。因此,Mao 等^[130]在集合卡尔曼滤波方法的基础上,进一步提出了一种双集成卡尔曼滤波的同化方法用于激光雷达数据的去噪与反演,在迭代过程中可以提供反馈函数,去噪效果和反演精度要优于单集合卡尔曼同化方法。

此外,人们开展了多方法联合去噪研究,通过联合形态滤波与经验模态分解^[131]、软阈值和粗糙度惩罚与集合经验模态分解^[132]、互补集合经验模态分解与小波阈值^[133]、基于集合经验模态分解的小波变换与局部加权散点平滑^[134]、小波变换与变分模态分解^[135]等多种不同方法,用于激光雷达回波信号的去噪并取得了较好的效果。单一的去噪方法有其自身的优点和缺点,而通过对不同方法进行联合,可以更好地发挥出不同方法的优势^[136]。此外,近年来流行的机器学习和深度学习等技术也在激光雷达信号降噪方面开展了一些应用,相比于传统的单一方法具有更好的去噪效果,但其依赖于大量的样本进行训练,相关方法还在发展阶段^[129, 137]。

总体上,激光雷达的抗噪方法主要有滑动平均法、频率分解法、同化滤波法、联合抗噪法和神经网络法等。其中滑动平均法难以适用于不平稳信号的处理。频率分解法中小波法相对可靠并在信号降噪中使用更加普遍。而经验模态分解法则存在模态混叠的问题,目前还不够成熟。同化滤波法考虑了激光雷达物理方程的约束,具有同时获得抗噪信号和反演结果的特点,具有一定的发展潜力。此外,联合抗噪算法理论上性能要优于单一方法,而新兴的神经网络法方法由于缺少足够的样本训练,因此目前使用仍然较少。

6 总结与展望

地基 Mie 激光雷达具有全天候、高时空分辨率探测大气垂直廓线信息的优势,获得了广泛的应用。目前已经发展出了大量提升激光雷达数据产品处理精度的方法,有力地推进了地基激光雷达的技术发展和研究应用。但在地基 Mie 散射激光雷达数据处理中仍然存在重叠因子修正、云和气溶胶层次检测和数据反演等关键问题:

1) 对于几何重叠因子带来的低空探测信号不全的问题,目前已经发展出了实验法、解析法和光线追踪法等修正方法。而双视场激光雷达和 CCD 侧向散射激光雷达等新型技术的发展,为低盲区甚至零盲区的激光雷达探测提供了更多的可能;

2) 对于云和气溶胶层次检测问题,目前已经发展出了斜率法、阈值法和假设检验等方法。斜率法和阈值法在目前激光雷达产品生产中广泛使用,但是仍然存在很多一刀切的经验判断,导致弱层次漏检的问题。而通过将层次检测转换为假设检验问题,可以实现更加精确的层次检测,在未来激光雷达产品生产中具有更大的应用潜力;

3) 对于激光雷达信号反演问题,目前主要存在边界值选择、激光雷达比确定和噪声干扰三个关键问题。在未来激光雷达反演中,边界值的选择需要尽量避免简单的假设,并且在理论计算中要区分气溶胶和大气分子两种成分的贡献;对于激光雷达比确定,通过联合其他观测进行约束求解可以一定程度上缓解该问题;在激光雷达信号的抗噪中,可供选择的方法相对较多,但是由于很难有同步的观测真值作为评估参考数据,因此如何客观评估去噪效果仍然是个问题。

此外,由于本文篇幅有限,除了上述提到的三个关键反演问题,还有一些关键反演和技术难题没有得到充分的回顾,例如激光雷达多重散射效应去除、云和气溶胶分类、云和气溶胶的粒径谱等参数的反演、激光雷达与其他传感器的协同观测和联合反演,以及激光雷达硬件的成本降低、性能提升和应用推广等。这些方面目前也取得了较多进展,同时仍然值得更加深入的研究和探讨。

参 考 文 献

- Pöschl U. Atmospheric aerosols: composition, transformation, climate and health effects[J]. *Angewandte Chemie International Edition*, 2005, 44(46): 7520-7540.
- 于思琪, 刘东, 徐继伟, 等. 激光雷达反演大气边界层高度的优化方法[J]. *光学学报*, 2021, 41(7): 0728002.
Yu S Q, Liu D, Xu J W, et al. Optimization method of retrieving atmospheric boundary layer height by lidar[J]. *Acta Optica Sinica*, 2021, 41(7): 0728002.
- Gong W, Li J, Mao F Y, et al. Comparison of simultaneous signals obtained from a dual-field-of-view lidar and its application to noise reduction based on empirical mode decomposition[J]. *Chinese Optics Letters*, 2011, 9(5): 050101.
- Gong W, Zhang J Y, Mao F Y, et al. Measurements for profiles of aerosol extinction coefficient, backscatter coefficient, and lidar ratio over Wuhan in China with Raman/Mie lidar[J]. *Chinese Optics Letters*, 2010, 8(6): 533-536.
- Immler F, Engelbart D, Schrems O. Fluorescence from atmospheric aerosol detected by a lidar indicates biogenic particles in the lowermost stratosphere[J]. *Atmospheric Chemistry and Physics*, 2005, 5(2): 345-355.
- 黄忠伟, 王雍恺, 闭建荣, 等. 气溶胶激光雷达的国内外研究进展与展望[J]. *遥感学报*, 2022, 26(5): 834-851.
Huang Z W, Wang Y K, Bi J R, et al. An overview of aerosol lidar: progress and prospect[J]. *National Remote Sensing Bulletin*, 2022, 26(5): 834-851.
- 刘东, 杨雨英, 周雨迪, 等. 大气遥感高光谱分辨率激光雷达研究进展[J]. *红外与激光工程*, 2015, 44(9): 2535-2546.
Liu D, Yang Y Y, Zhou Y D, et al. High spectral resolution lidar for atmosphere remote sensing: a review[J]. *Infrared and Laser Engineering*, 2015, 44(9): 2535-2546.
- 张与鹏, 刘东, 杨雨英, 等. 近红外高光谱分辨率激光雷达光谱滤光器性能分析[J]. *中国激光*, 2016, 43(4): 0414004.
Zhang Y P, Liu D, Yang Y Y, et al. Spectrum filter performance analysis on near-infrared HighSpectral-resolution lidar[J]. *Chinese Journal of Lasers*, 2016, 43(4): 0414004.
- 成中涛. 基于视场展宽迈克尔逊干涉仪的高光谱分辨率激光雷达[D]. 杭州: 浙江大学, 2017.
Cheng Z T. High spectral resolution lidar based on Michelson interferometer with broadened field of view[D]. Hangzhou: Zhejiang University, 2017.
- 狄慧鸽, 华杭波, 张佳琪, 等. 高光谱分辨率激光雷达鉴频器的设计与分析[J]. *物理学报*, 2017, 66(18): 184202.
Di H G, Hua H B, Zhang J Q, et al. Design and analysis of high-spectral resolution lidar discriminator[J]. *Acta Physica Sinica*, 2017, 66(18): 184202.
- 周煜东. 基于LD的780 nm高光谱分辨率激光雷达系统设计[D]. 西安: 西安理工大学, 2020.
Zhou Y D. Design of 780 nm high spectral resolution lidar system based on LD[D]. Xi'an: Xi'an University of Technology, 2020.
- 沈雪. 高光谱分辨率激光雷达关键技术及系统实验[D]. 杭州: 浙江大学, 2021.
Shen X. Key technology and system experiment of hyperspectral resolution lidar[D]. Hangzhou: Zhejiang University, 2021.
- 朱首正, 卜令兵, 刘继桥, 等. 机载高光谱分辨率激光雷达探测大气气溶胶光学特性及污染研究[J]. *中国激光*, 2021, 48(17): 1710003.
Zhu S Z, Bu L B, Liu J Q, et al. Study on optical characteristics and pollution of atmospheric aerosol detected by airborne hyperspectral resolution lidar[J]. *Chinese Journal of Lasers*, 2021, 48(17): 1710003.
- Lohmann U, Feichter J. Global indirect aerosol effects: a review[J]. *Atmospheric Chemistry and Physics*, 2005, 5(3): 715-737.
- Jiang Y B, Froidevaux L, Lambert A, et al. Validation of aura microwave limb sounder ozone by ozonesonde and lidar measurements[J]. *Journal of Geophysical Research: Atmospheres*, 2007, 112(D24): D24S34.
- Fiocco G, Smullin L D. Detection of scattering layers in the upper atmosphere (60 - 140 km) by optical radar[J]. *Nature*, 1963, 199(4900): 1275-1276.
- 邱金桓, 吕达仁, 陈洪滨, 等. 现代大气物理学研究进展[J]. *大气科学*, 2003, 27(4): 628-652.
Qiu J H, Lü D R, Chen H B, et al. Modern research progresses in atmospheric physics[J]. *Chinese Journal of Atmospheric Sciences*, 2003, 27(4): 628-652.
- 周军, 岳古明, 戚福第, 等. 大气气溶胶光学特性激光雷达探测[J]. *量子电子学报*, 1998, 15(2): 140-148.
Zhou J, Yue G M, Qi F D, et al. Optical properties of aerosol derived from lidar measurements[J]. *Chinese Journal of Quantum Electronics*, 1998, 15(2): 140-148.
- 杨昭, 李强, 孙东松. 基于1064 nm米散射激光雷达的大气消光特性的研究[J]. *激光技术*, 2006, 30(2): 170-173.
Yang Z, Li Q, Sun D S. Study about atmosphere extinction coefficient based on 1064 nm Mie-scattering lidar[J]. *Laser Technology*, 2006, 30(2): 170-173.
- 张改霞, 赵曰峰, 张寅超, 等. 激光雷达白天探测大气边界层气溶胶[J]. *物理学报*, 2008, 57(11): 7390-7395.
Zhang G X, Zhao Y F, Zhang Y C, et al. A lidar system for monitoring planetary boundary layer aerosol in daytime[J]. *Acta Physica Sinica*, 2008, 57(11): 7390-7395.
- Schotland R M, Sassen K, Stone R. Observations by lidar of linear depolarization ratios for hydrometeors[J]. *Journal of Applied Meteorology*, 1971, 10(5): 1011-1017.
- Pal S R, Carswell A I. Polarization properties of lidar scattering from clouds at 347 nm and 694 nm[J]. *Applied Optics*, 1978, 17(15): 2321-2328.
- Iwasaka Y, Hayashida S. The effects of the volcanic eruption of St. Helens on the polarization properties of stratospheric

- aerosols; lidar measurement at Nagoya[J]. Journal of the Meteorological Society of Japan Ser II, 1981, 59(4): 611-614.
- [24] Sasano Y, Browell E V. Light scattering characteristics of various aerosol types derived from multiple wavelength lidar observations[J]. Applied Optics, 1989, 28(9): 1670-1679.
- [25] 周军, 岳古明, 金传佳, 等. 探测对流层气溶胶的双波长米氏散射激光雷达[J]. 光学学报, 2000, 20(10): 1412-1417.
Zhou J, Yue G M, Jin C J, et al. Two-wavelength Mie lidar for monitoring of tropospheric aerosol[J]. Acta Optica Sinica, 2000, 20(10): 1412-1417.
- [26] 迟如利, 吴德成, 刘博, 等. 双波长米氏散射激光雷达探测对流层气溶胶消光特性[J]. 光谱学与光谱分析, 2009, 29(6): 1468-1472.
Chi R L, Wu D C, Liu B, et al. Dual-wavelength Mie lidar observations of tropospheric aerosols[J]. Spectroscopy and Spectral Analysis, 2009, 29(6): 1468-1472.
- [27] 钟志庆, 刘博, 范爱媛, 等. 双波长双视场米氏散射激光雷达[J]. 大气与环境光学学报, 2008, 3(3): 173-178.
Zhong Z Q, Liu B, Fan A Y, et al. Two-wavelength Mie lidar with two receivers[J]. Journal of Atmospheric and Environmental Optics, 2008, 3(3): 173-178.
- [28] 邱金桓, 郑斯平, 黄其荣, 等. 北京地区对流层中上部云和气溶胶的激光雷达探测[J]. 大气科学, 2003, 27(1): 1-7.
Qiu J H, Zheng S P, Huang Q R, et al. Lidar measurements of cloud and aerosol in the upper troposphere in Beijing[J]. Chinese Journal of Atmospheric Sciences, 2003, 27(1): 1-7.
- [29] 毛建东, 华灯鑫, 何廷尧, 等. 银川上空大气气溶胶光学特性激光雷达探测研究[J]. 光谱学与光谱分析, 2010, 30(7): 2006-2010.
Mao J D, Hua D X, He T Y, et al. Lidar observations of atmospheric aerosol optical properties over Yinchuan area[J]. Spectroscopy and Spectral Analysis, 2010, 30(7): 2006-2010.
- [30] 毛敏娟, 吴永华, 戚福弟, 等. 车载式 1064 nm 和 532 nm 双波长米氏散射激光雷达[J]. 强激光与粒子束, 2005, 17(5): 677-680.
Mao M J, Wu Y H, Qi F D, et al. Mobile dual-wavelength Mie lidar[J]. High Power Laser and Particle Beams, 2005, 17(5): 677-680.
- [31] 赵虎, 华灯鑫, 狄慧鸽, 等. 全天时多波长激光雷达系统研制与信噪比分析[J]. 中国激光, 2015, 42(1): 0113001.
Zhao H, Hua D X, Di H G, et al. Development of all time multi-wavelength lidar system and analysis of its signal to noise ratio[J]. Chinese Journal of Lasers, 2015, 42(1): 0113001.
- [32] 狄慧鸽, 侯晓龙, 赵虎, 等. 多波长激光雷达探测多种天气气溶胶光学特性与分析[J]. 物理学报, 2014, 63(24): 244206.
Di H G, Hou X L, Zhao H, et al. Detections and analyses of aerosol optical properties under different weather conditions using multi-wavelength Mie lidar[J]. Acta Physica Sinica, 2014, 63(24): 244206.
- [33] 刘东, 戚福弟, 金传佳, 等. 合肥上空卷云和沙尘气溶胶退偏振比的激光雷达探测[J]. 大气科学, 2003, 27(6): 1093-1100.
Liu D, Qi F D, Jin C J, et al. Polarization lidar observations of cirrus clouds and Asian dust aerosols over Hefei[J]. Chinese Journal of Atmospheric Sciences, 2003, 27(6): 1093-1100.
- [34] 迟如利, 刘厚通, 王珍珠, 等. 偏振-米氏散射激光雷达对卷云的探测[J]. 强激光与粒子束, 2009, 21(9): 1295-1300.
Chi R L, Liu H T, Wang Z Z, et al. Observations of cirrus clouds using polarization Mie lidar[J]. High Power Laser and Particle Beams, 2009, 21(9): 1295-1300.
- [35] 潘昱冰, 吕达仁, 潘蔚琳, 等. 地基双波长偏振激光雷达对格尔木地区卷云观测的个例研究[J]. 气候与环境研究, 2015, 20(5): 581-588.
Pan Y B, Lü D R, Pan W L, et al. A case study of cirrus cloud over Geermu city using two-wavelength polarization lidar[J]. Climatic and Environmental Research, 2015, 20(5): 581-588.
- [36] Misra A, Tripathi S N, Kaul D S, et al. Study of MPLNET-derived aerosol climatology over Kanpur, India, and validation of CALIPSO level 2 version 3 backscatter and extinction products[J]. Journal of Atmospheric and Oceanic Technology, 2012, 29(9): 1285-1294.
- [37] Wandinger U, Freudenthaler V, Baars H, et al. EARLINET instrument intercomparison campaigns: overview on strategy and results[J]. Atmospheric Measurement Techniques, 2016, 9(3): 1001-1023.
- [38] De Mazière M, Thompson A M, Kurylo M J, et al. The Network for the Detection of Atmospheric Composition Change (NDACC): history, status and perspectives[J]. Atmospheric Chemistry and Physics, 2018, 18(7): 4935-4964.
- [39] Shimizu A, Nishizawa T, Jin Y, et al. Evolution of a lidar network for tropospheric aerosol detection in East Asia[J]. Optical Engineering, 2016, 56(3): 031219.
- [40] Guerrero-Rascado J L, Landulfo E, Antuña J C, et al. Latin American lidar network (LALINET) for aerosol research: diagnosis on network instrumentation[J]. Journal of Atmospheric and Solar-Terrestrial Physics, 2016, 138/139: 112-120.
- [41] 田晓敏, 刘东, 徐继伟, 等. 大气探测激光雷达网络和星载激光雷达技术综述[J]. 大气与环境光学学报, 2018, 13(6): 401-416.
Tian X M, Liu D, Xu J W, et al. Review on atmospheric detection lidar network and spaceborne lidar technology[J]. Journal of Atmospheric and Environmental Optics, 2018, 13(6): 401-416.
- [42] Zuev V V, Burlakov V D, Nevzorov A V, et al. 30-year lidar observations of the stratospheric aerosol layer state over Tomsk (Western Siberia, Russia) [J]. Atmospheric Chemistry and Physics, 2017, 17(4): 3067-3081.
- [43] 袁林, 刘博, 王邦新, 等. 车载式 1064 nm 米氏散射激光雷达的研制[J]. 中国激光, 2010, 37(7): 1721-1725.
Yuan L, Liu B, Wang B X, et al. Design of mobile 1064 nm Mie scattering lidar[J]. Chinese Journal of Lasers, 2010, 37(7): 1721-1725.
- [44] 王界, 刘文清, 张天舒, 等. 便携式双视场米氏散射激光雷达系统的研制[J]. 仪器仪表学报, 2019, 40(2): 148-154.
Wang J, Liu W Q, Zhang T S, et al. Development of a portable dual field-of-view Mie-scattering Lidar[J]. Chinese Journal of Scientific Instrument, 2019, 40(2): 148-154.
- [45] Kamei A, Sugimoto N, Matsui I, et al. Volcanic aerosol layer observed by shipboard lidar over the tropical western Pacific[J]. SOLA, 2006, 2: 1-4.
- [46] Fernald F G, Herman B M, Reagan J A. Determination of aerosol height distributions by lidar[J]. Journal of Applied Meteorology, 1972, 11(3): 482-489.
- [47] Stelmaszczyk K, Dell'Aglio M, Chudzyński S, et al. Analytical function for lidar geometrical compression form-factor calculations[J]. Applied Optics, 2005, 44(7): 1323-1331.
- [48] 王威, 毛飞跃, 龚威, 等. 基于激光强度分布的激光雷达重叠因子计算及其敏感性分析[J]. 光学学报, 2014, 34(2): 0228005.
Wang W, Mao F Y, Gong W, et al. Overlap factor calculation method based on laser intensity distribution and its sensitivity analysis[J]. Acta Optica Sinica, 2014, 34(2): 0228005.
- [49] Sasano Y, Shimizu H, Takeuchi N, et al. Geometrical form factor in the laser radar equation: an experimental determination [J]. Applied Optics, 1979, 18(23): 3908-3910.
- [50] Su J, McCormick M P, Liu Z Y, et al. Obtaining a ground-based lidar geometric form factor using coincident spaceborne lidar measurements[J]. Applied Optics, 2010, 49(1): 108-113.
- [51] 肖韶荣, 龙强, 周洁, 等. 非共轴激光雷达消光反演中参考高度的标定[J]. 现代雷达, 2012, 34(11): 84-88.
Xiao S R, Long Q, Zhou J, et al. Calibration of reference height in the inversion extinction coefficient for non coaxial laser radar [J]. Modern Radar, 2012, 34(11): 84-88.
- [52] Halldórsson T, Langerholc J. Geometrical form factors for the lidar function[J]. Applied Optics, 1978, 17(2): 240-244.
- [53] Sassen K, Dodd G C. Lidar crossover function and misalignment effects[J]. Applied Optics, 1982, 21(17): 3162-

- 3165.
- [54] Liu B, Yi F, Yu C M. Methods for optical adjustment in lidar systems[J]. *Applied Optics*, 2005, 44(8): 1480-1484.
- [55] Bereznyy I. A combined diffraction and geometrical optics approach for lidar overlap function computation[J]. *Optics and Lasers in Engineering*, 2009, 47(7/8): 855-859.
- [56] Velotta R, Bartoli B, Capobianco R, et al. Analysis of the receiver response in lidar measurements[J]. *Applied Optics*, 1998, 37(30): 6999-7007.
- [57] 刘巧君, 杨林, 王劫予, 等. 基于激光器输出模式的离轴激光雷达重叠因子计算及近场信号校正[J]. *物理学报*, 2009, 58(10): 7376-7381.
Liu Q J, Yang L, Wang J Y, et al. Calculation of the overlap factor and correction of near-field signal of the off-axis lidar based on the Gaussian mode of laser beam[J]. *Acta Physica Sinica*, 2009, 58(10): 7376-7381.
- [58] 狄慧鸽, 华灯鑫, 王玉峰, 等. 米散射激光雷达重叠因子及全程回波信号标定技术研究[J]. *物理学报*, 2013, 62(9): 094215.
Di H G, Hua D X, Wang Y F, et al. Investigation on the correction of the Mie scattering lidar's overlapping factor and echo signals over the total detection range? [J]. *Acta Physica Sinica*, 2013, 62(9): 094215.
- [59] Wandinger U, Ansmann A. Experimental determination of the lidar overlap profile with Raman lidar[J]. *Applied Optics*, 2002, 41(3): 511-514.
- [60] Guerrero-Rascado J L, Costa M J, Bortoli D, et al. Infrared lidar overlap function: an experimental determination[J]. *Optics Express*, 2010, 18(19): 20350-20359.
- [61] 张寅超, 王立福, 王琛, 等. 基于光线追迹非同轴激光雷达重叠因子影响因素的分析研究[J]. *北京理工大学学报*, 2023, 43(2): 213-220.
Zhang Y C, Wang L F, Wang C, et al. Analysis and research on influencing factors of non-coaxial lidar overlap factor based on ray tracing[J]. *Transactions of Beijing Institute of Technology*, 2023, 43(2): 213-220.
- [62] Gong W, Mao F Y, Li J. OFLID: simple method of overlap factor calculation with laser intensity distribution for biaxial lidar [J]. *Optics Communications*, 2011, 284(12): 2966-2971.
- [63] Mao F Y, Gong W, Li J. Geometrical form factor calculation using Monte Carlo integration for lidar[J]. *Optics & Laser Technology*, 2012, 44(4): 907-912.
- [64] Wang J, Liu W Q, Liu C, et al. The determination of aerosol distribution by a No-blind-zone scanning lidar[J]. *Remote Sensing*, 2020, 12(4): 626.
- [65] 李俊, 龚威, 毛飞跃, 等. 探测武汉上空大气气溶胶的双视场激光雷达[J]. *光学学报*, 2013, 33(12): 1201001.
Li J, Gong W, Mao F Y, et al. Dual field of view lidar for observing atmospheric aerosols over Wuhan[J]. *Acta Optica Sinica*, 2013, 33(12): 1201001.
- [66] 王界. 双视场零盲区激光雷达的研制及应用[D]. 合肥: 中国科学技术大学, 2020.
Wang J. Development and application of double field of view and zero blind area lidar[D]. Hefei: University of Science and Technology of China, 2020.
- [67] 黄立峰, 龚威, 李俊, 等. 大气遥感双视场米散射激光雷达信号拼接[J]. *遥感学报*, 2012, 16(4): 705-719.
Huang L F, Gong W, Li J, et al. Signal splicing of dual-receiver Mie scattering lidar in atmospheric remote sensing[J]. *Journal of Remote Sensing*, 2012, 16(4): 705-719.
- [68] 麻晓敏, 陶宗明, 张璐璐, 等. 侧向散射激光雷达探测白天近地面气溶胶探测技术[J]. *光学学报*, 2018, 38(4): 0401005.
Ma X M, Tao Z M, Zhang L L, et al. Ground layer aerosol detection technology during daytime based on side-scattering lidar[J]. *Acta Optica Sinica*, 2018, 38(4): 0401005.
- [69] 狄慧鸽, 华灯鑫. 底层大气探测激光雷达国内研究现状与进展(特邀)[J]. *红外与激光工程*, 2021, 50(3): 20210032.
Di H G, Hua D X. Research status and progress of Lidar for atmosphere in China(Invited)[J]. *Infrared and Laser Engineering*, 2021, 50(3): 20210032.
- [70] Pal S R, Steinbrecht W, Carswell A I. Automated method for lidar determination of cloud-base height and vertical extent[J]. *Applied Optics*, 1992, 31(10): 1488-1494.
- [71] Wang Z E, Sassen K. Cloud type and macrophysical property retrieval using multiple remote sensors[J]. *Journal of Applied Meteorology*, 2001, 40(10): 1665-1682.
- [72] Kovalev V A, Newton J, Wold C, et al. Simple algorithm to determine the near-edge smoke boundaries with scanning lidar [J]. *Applied Optics*, 2005, 44(9): 1761-1768.
- [73] Cromwell E, Flynn D. Lidar cloud detection with fully convolutional networks[C]//2019 IEEE Winter Conference on Applications of Computer Vision (WACV), January 7-11, 2019, Waikoloa, HI, USA. New York: IEEE Press, 2019: 619-627.
- [74] Morille Y, Haeffelin M, Drobinski P, et al. STRAT: an automated algorithm to retrieve the vertical structure of the atmosphere from single-channel lidar data[J]. *Journal of Atmospheric and Oceanic Technology*, 2007, 24(5): 761-775.
- [75] Mao F Y, Gong W, Zhu Z M. Simple multiscale algorithm for layer detection with lidar[J]. *Applied Optics*, 2011, 50(36): 6591-6598.
- [76] 陈思颖, 王嘉奇, 陈和, 等. 改进简单多尺度法的激光雷达云检测[J]. *红外与激光工程*, 2020, 49(S2): 20200379.
Chen S Y, Wang J Q, Chen H, et al. Lidar cloud detection based on improved simple multiscale method[J]. *Infrared and Laser Engineering*, 2020, 49(S2): 20200379.
- [77] Young S A. Analysis of lidar backscatter profiles in optically thin clouds[J]. *Applied Optics*, 1995, 34(30): 7019-7031.
- [78] Vaughan M A, Powell K A, Winker D M, et al. Fully automated detection of cloud and aerosol layers in the CALIPSO lidar measurements[J]. *Journal of Atmospheric and Oceanic Technology*, 2009, 26(10): 2034-2050.
- [79] Rogers R R, Vaughan M A, Hostetler C A, et al. Looking through the haze: evaluating the CALIPSO level 2 aerosol optical depth using airborne high spectral resolution lidar data[J]. *Atmospheric Measurement Techniques*, 2014, 7(12): 4317-4340.
- [80] Kim M H, Omar A H, Vaughan M A, et al. Quantifying the low bias of CALIPSO's column aerosol optical depth due to undetected aerosol layers[J]. *Journal of Geophysical Research. Atmospheres: JGR*, 2017, 122(2): 1098-1113.
- [81] Lewis J R, Campbell J R, Welton E J, et al. Overview of MPLNET version 3 cloud detection[J]. *Journal of Atmospheric and Oceanic Technology*, 2016, 33(10): 2113-2134.
- [82] Xu W W, Zhang Y C, Mao F Y, et al. Joint multiscale cloud detection algorithm for ground-based lidar[J]. *Optics Express*, 2022, 30(25): 44449-44463.
- [83] Mao F Y, Liang Z X, Pan Z X, et al. A simple multiscale layer detection algorithm for CALIPSO measurements[J]. *Remote Sensing of Environment*, 2021, 266: 112687.
- [84] Collis R T H. Lidar: a new atmospheric probe[J]. *Quarterly Journal of the Royal Meteorological Society*, 1966, 92(392): 220-230.
- [85] Klett J D. Stable analytical inversion solution for processing lidar returns[J]. *Applied Optics*, 1981, 20(2): 211-220.
- [86] Fernald F G. Analysis of atmospheric lidar observations: some comments[J]. *Applied Optics*, 1984, 23(5): 652-653.
- [87] Rocadenbosch F, Soriano C, Comerón A, et al. Lidar inversion of atmospheric backscatter and extinction-to-backscatter ratios by use of a Kalman filter[J]. *Applied Optics*, 1999, 38(15): 3175-3189.
- [88] Kovalev V A. Stable near-end solution of the lidar equation for clear atmospheres[J]. *Applied Optics*, 2003, 42(3): 585-591.
- [89] Rocadenbosch F, Comerón A, Pineda D. Assessment of lidar inversion errors for homogeneous atmospheres[J]. *Applied*

- Optics, 1998, 37(12): 2199-2206.
- [90] Sasano Y, Browell E V, Ismail S. Error caused by using a constant extinction/backscattering ratio in the lidar solution[J]. Applied Optics, 1985, 24(22): 3929-3932.
- [91] Sasano Y. Tropospheric aerosol extinction coefficient profiles derived from scanning lidar measurements over Tsukuba, Japan, from 1990 to 1993[J]. Applied Optics, 1996, 35(24): 4941-4952.
- [92] Mao F Y, Shi R X, Rosenfeld D, et al. Retrieving instantaneous extinction of aerosol undetected by the CALIPSO layer detection algorithm[J]. Atmospheric Chemistry and Physics, 2022, 22(16): 10589-10602.
- [93] Kunz G J, de Leeuw G. Inversion of lidar signals with the slope method[J]. Applied Optics, 1993, 32(18): 3249-3256.
- [94] Rocadenbosch F, Comerón A, Albiol L. Statistics of the slope-method estimator[J]. Applied Optics, 2000, 39(33): 6049-6057.
- [95] 田鹏飞, 张镭, 曹贤洁, 等. 基于 Fernald 和 Klett 方法确定气溶胶消光系数边界值[J]. 量子电子学报, 2013, 30(1): 57-65.
Tian P F, Zhang L, Cao X J, et al. A novel approach based on Fernald's and Klett's method to determine the atmospheric extinction coefficient boundary value[J]. Chinese Journal of Quantum Electronics, 2013, 30(1): 57-65.
- [96] 熊兴隆, 冯帅, 蒋立辉, 等. 一种新的大气消光系数边界值确定方法[J]. 光电子·激光, 2011, 22(11): 1699-1705.
Xiong X L, Feng S, Jiang L H, et al. A novel method for determining the boundary value of the atmospheric extinction coefficient[J]. Journal of Optoelectronics·Laser, 2011, 22(11): 1699-1705.
- [97] 贺应红, 郑玉臣, 程娟, 等. 最小二乘法拟合大气激光雷达回波信号估算消光系数边界值[J]. 量子电子学报, 2004, 21(6): 879-883.
He Y H, Zheng Y C, Cheng J, et al. Estimation of extinction efficient boundary value with least-square fitting for lidar return signal[J]. Chinese Journal of Quantum Electronics, 2004, 21(6): 879-883.
- [98] 杨彬, 莫祖斯, 刘海姣, 等. 大气探测激光雷达突变信号处理方法研究(特邀)[J]. 红外与激光工程, 2022, 51(1): 20211117.
Yang B, Mo Z S, Liu H J, et al. Study on abrupt signal processing method of atmospheric lidar(Invited)[J]. Infrared and Laser Engineering, 2022, 51(1): 20211117.
- [99] 熊兴隆, 蒋立辉, 冯帅, 等. 基于不动点原理的大气气溶胶消光系数边界值确定方法[J]. 光电子·激光, 2012, 23(2): 303-309.
Xiong X L, Jiang L H, Feng S, et al. Determination of the boundary value of atmospheric aerosol extinction coefficient based on fixed point principle[J]. Journal of Optoelectronics·Laser, 2012, 23(2): 303-309.
- [100] 熊兴隆, 蒋立辉, 冯帅, 等. 改进的牛顿法确定大气消光系数边界值[J]. 红外与激光工程, 2012, 41(7): 1744-1749.
Xiong X L, Jiang L H, Feng S, et al. Using improved Newton method to determine the boundary value of atmospheric extinction coefficient[J]. Infrared and Laser Engineering, 2012, 41(7): 1744-1749.
- [101] 孙国栋, 秦来安, 张巴龙, 等. 一种测量大气消光系数边界值的新方法[J]. 物理学报, 2018, 67(5): 054205.
Sun G D, Qin L A, Zhang S L, et al. A new method of measuring boundary value of atmospheric extinction coefficient [J]. Acta Physica Sinica, 2018, 67(5): 054205.
- [102] 陈涛, 吴德成, 刘博, 等. 低层大气中确定气溶胶后向散射系数边界值的新方法[J]. 光学学报, 2010, 30(6): 1531-1536.
Chen T, Wu D C, Liu B, et al. A new method for determining aerosol backscatter coefficient boundary value in the lower troposphere[J]. Acta Optica Sinica, 2010, 30(6): 1531-1536.
- [103] Ma Y Z, Liu J Q, Chen N, et al. Determination of the boundary value of the aerosol extinction coefficient and its effects on the extinction coefficient profile of aerosol in lower atmosphere[J]. Optik, 2018, 160: 283-297.
- [104] Tao Z M, Zhang Q Z, Yuan K E, et al. Retrieving aerosol backscattering coefficient for short range lidar using parameter selection at reference point[J]. Chinese Optics Letters, 2010, 8(8): 732.
- [105] Mao F Y, Wang W, Min Q L, et al. Approach for selecting boundary value to retrieve Mie-scattering lidar data based on segmentation and two-component fitting methods[J]. Optics Express, 2015, 23(11): A604-A613.
- [106] 张寅超, 陈粟, 檀望舒, 等. 以水云后向散射系数为边界值的激光雷达气溶胶后向散射系数反演方法[J]. 光学学报, 2022, 42(24): 2428002.
Zhang Y C, Chen S, Tan W S, et al. Inversion algorithm of aerosol backscattering coefficient with water cloud particle backscattering coefficient as boundary value[J]. Acta Optica Sinica, 2022, 42(24): 2428002.
- [107] Wiegner M, Groß S, Freudenthaler V, et al. The May/June 2008 Saharan dust event over Munich: intensive aerosol parameters from lidar measurements[J]. Journal of Geophysical Research: Atmospheres, 2011, 116(D23): D23213.
- [108] Omar A H, Won J G, Winker D M, et al. Development of global aerosol models using cluster analysis of Aerosol Robotic Network (AERONET) measurements[J]. Journal of Geophysical Research, 2005, 110(D10): D10S14.
- [109] 张朝阳, 苏林, 陈良富. 中国典型地区气溶胶激光雷达比反演与分析[J]. 中国激光, 2013, 40(5): 0513002.
Zhang Z Y, Su L, et al. Retrieval and analysis of aerosol lidar ratio at several typical regions in China[J]. Chinese Journal of Lasers, 2013, 40(5): 0513002.
- [110] Kim M H, Omar A H, Tackett J L, et al. The CALIPSO version 4 automated aerosol classification and lidar ratio selection algorithm[J]. Atmospheric Measurement Techniques, 2018, 11(11): 6107-6135.
- [111] Huang Z W, Huang J P, Bi J R, et al. Dust aerosol vertical structure measurements using three MPL lidars during 2008 China-U.S. joint dust field experiment[J]. Journal of Geophysical Research, 2010, 115(D7): D00K15.
- [112] 宋跃辉, 时丽丽, 王玉峰, 等. 气溶胶激光雷达比的迭代反演[J]. 中国激光, 2016, 43(1): 0113001.
Song Y H, Shi L L, Wang Y F, et al. Retrieve of lidar ratio of aerosols by iteration[J]. Chinese Journal of Lasers, 2016, 43(1): 0113001.
- [113] Cuesta J, Flamant P H, Flamant C. Synergetic technique combining elastic backscatter lidar data and sunphotometer AERONET inversion for retrieval by layer of aerosol optical and microphysical properties[J]. Applied Optics, 2008, 47(25): 4598-4611.
- [114] 包青, 贺军亮, 查勇. 基于动态雷达比的气溶胶消光系数及光学厚度反演[J]. 光学学报, 2015, 35(3): 0301002.
Bao Q, He J L, Zha Y. Retrieval of aerosol extinction coefficient and optical thickness using varied lidar ratio[J]. Acta Optica Sinica, 2015, 35(3): 0301002.
- [115] 华雯丽, 韩颖, 乔瀚洋, 等. 敦煌沙尘气溶胶质量浓度垂直特征个例分析[J]. 高原气象, 2018, 37(5): 1428-1439.
Hua W L, Han Y, Qiao H Y, et al. Profiling of dust aerosol mass concentration over Dunhuang: case studies[J]. Plateau Meteorology, 2018, 37(5): 1428-1439.
- [116] Wang X, Frontoso M G, Pisani G, et al. Retrieval of atmospheric particles optical properties by combining ground-based and spaceborne lidar elastic scattering profiles[J]. Optics Express, 2007, 15(11): 6734-6743.
- [117] Su J, Liu Z Y, Wu Y H, et al. Retrieval of multi-wavelength aerosol lidar ratio profiles using Raman scattering and Mie backscattering signals[J]. Atmospheric Environment, 2013, 79: 36-40.
- [118] 沈吉, 曹念文. 米-拉曼散射激光雷达反演对流层气溶胶消光系数廓线[J]. 中国激光, 2017, 44(6): 0610003.
Shen J, Cao N. Inversion of tropospheric aerosol extinction

- coefficient profile by Mie-Raman scattering lidar[J]. Chinese Journal of Lasers, 2017, 44(6): 0610003.
- [119] Fang H T, Huang D S. Noise reduction in lidar signal based on discrete wavelet transform[J]. Optics Communications, 2004, 233(1/2/3): 67-76.
- [120] Fang H T, Huang D S, Wu Y H. Antinoise approximation of the lidar signal with wavelet neural networks[J]. Applied Optics, 2005, 44(6): 1077-1083.
- [121] Mao F Y, Gong W, Li C. Anti-noise algorithm of lidar data retrieval by combining the ensemble Kalman filter and the Fernald method[J]. Optics Express, 2013, 21(7): 8286-8297.
- [122] Wu S H, Liu Z S, Liu B Y. Enhancement of lidar backscatters signal-to-noise ratio using empirical mode decomposition method [J]. Optics Communications, 2006, 267(1): 137-144.
- [123] Zhou Z R, Hua D X, Wang Y F, et al. Improvement of the signal to noise ratio of Lidar echo signal based on wavelet denoising technique[J]. Optics and Lasers in Engineering, 2013, 51(8): 961-966.
- [124] Huang N E, Shen Z, Long S R, et al. The empirical mode decomposition and the Hilbert spectrum for nonlinear and non-stationary time series analysis[J]. Proceedings of the Royal Society of London Series A: Mathematical, Physical and Engineering Sciences, 1998, 454(1971): 903-995.
- [125] Tian P F, Cao X J, Liang J N, et al. Improved empirical mode decomposition based denoising method for lidar signals[J]. Optics Communications, 2014, 325: 54-59.
- [126] Wu Z H, Huang N E. Ensemble empirical mode decomposition: a noise-assisted data analysis method[J]. Advances in Adaptive Data Analysis, 2009, 1(1): 1-41.
- [127] 徐帆, 常建华, 刘秉刚, 等. 基于 VMD 的激光雷达回波信号去噪方法研究[J]. 激光与红外, 2018, 48(11): 1443-1448.
- Xu F, Chang J H, Liu B G, et al. De-noising method research for lidar echo signal based on variational mode decomposition[J]. Laser & Infrared, 2018, 48(11): 1443-1448.
- [128] Li C, Pan Z X, Mao F Y, et al. De-noising and retrieving algorithm of Mie lidar data based on the particle filter and the Fernald method[J]. Optics Express, 2015, 23(20): 26509-26520.
- [129] Zeng X J, Guo W P, Yang K C, et al. Noise reduction and retrieval by modified lidar inversion method combines joint retrieval method and machine learning[J]. Applied Physics B, 2018, 124(12): 238.
- [130] Mao F Y, Liu J, Wang L, et al. Denoising and retrieval algorithm based on a dual ensemble Kalman filter for elastic lidar data[J]. Optics Communications, 2019, 433: 137-143.
- [131] 蒋立辉, 符超, 刘雯箐, 等. 基于自适应多尺度形态滤波与 EMD 的激光雷达回波信号去噪方法[J]. 红外与激光工程, 2015, 44(5): 1673-1679.
- Jiang L H, Fu C, Liu W Q, et al. Lidar backscattering signal denoising method based on adaptive multi-scale morphological filtering and EMD[J]. Infrared and Laser Engineering, 2015, 44(5): 1673-1679.
- [132] Chang J H, Zhu L Y, Li H X, et al. Noise reduction in Lidar signal using correlation-based EMD combined with soft thresholding and roughness penalty[J]. Optics Communications, 2018, 407: 290-295.
- [133] 马愈昭, 刘逵, 张岩峰, 等. CEEMD 结合改进小波阈值的激光雷达信号去噪算法[J]. 系统工程与电子技术, 2023, 45(1): 93-100.
- Ma Y Z, Liu K, Zhang Y F, et al. Laser radar signal denoising algorithm based on CEEMD combined with improved wavelet threshold[J]. Systems Engineering and Electronics, 2023, 45(1): 93-100.
- [134] Zhang Y J, Wu T, Zhang X Z, et al. Rayleigh lidar signal denoising method combined with WT, EEMD and LOWESS to improve retrieval accuracy[J]. Remote Sensing, 2022, 14(14): 3270.
- [135] Wang Z Z, Ding H B, Wang B X, et al. New denoising method for lidar signal by the WT-VMD joint algorithm[J]. Sensors, 2022, 22(16): 5978.
- [136] 丁红波, 王珍珠, 刘东. 激光雷达信号去噪方法的对比研究[J]. 光学学报, 2021, 41(24): 2401001.
- Ding H B, Wang Z Z, Liu D. Comparison of de-noising methods of LiDAR signal[J]. Acta Optica Sinica, 2021, 41(24): 2401001.
- [137] Hu M H, Mao J D, Li J, et al. A novel lidar signal denoising method based on convolutional autoencoding deep learning neural network[J]. Atmosphere, 2021, 12(11): 1403.

Research Progress and Challenges in Retrieval of Ground-Based Mie Scattering Lidar

Mao Feiyue^{1,2}, Xu Weiwei¹, Zang Lin³, Pan Zengxin^{2,4}, Gong Wei^{2,3*}

¹School of Remote Sensing and Information Engineering, Wuhan University, Wuhan 430079, Hubei, China;

²State Key Laboratory of Information Engineering in Surveying, Mapping and Remote Sensing, Wuhan University, Wuhan 430079, Hubei, China;

³Electronic Information School, Wuhan University, Wuhan 430079, Hubei, China;

⁴Institute of Earth Sciences, The Hebrew University of Jerusalem, Jerusalem 91904, Israel

Abstract

Significance Aerosols and clouds are important components of the earth-atmosphere system with intricate physical, chemical, and optical properties. They have a significant influence on the atmospheric environment, climate change, and human health. Observing and studying the properties of aerosols and clouds are of great significance to gain insight into these issues. Currently, remote sensing technologies and methods are widely developed to observe aerosol and cloud properties, such as optical depth, extinction coefficient, and particle size distribution.

Lidar is one of the most useful active remote sensing tools due to its ability to detect the vertical distribution of the

atmosphere. Among various types of lidars, ground-based Mie scattering lidar is the most popular one for cloud and aerosol detection with strong echo signals, simple system structure, and easy implementation. The development of Mie lidar began in the 1960s, and later multi-wavelength and polarization techniques were developed to more comprehensively detect scattering properties and particle sizes of aerosols and clouds. Nowadays, many lidar networks have been established for regional and global atmospheric environmental monitoring.

As the ground-based Mie lidar is becoming widespread, accurately retrieving their data is urgently required. However, retrieval is still facing many challenges that lead to large uncertainties. First, the correction of the overlap factor is crucial because the near-surface atmospheric information is often the most concerned. Second, the identification and extraction of cloud and aerosol layers from noisy lidar signals are essential for subsequent optical parameter retrieval and atmospheric research. Finally, data retrieval is a key step in lidar signal processing as it reveals the optical properties of aerosols and clouds. Hence, we mainly review the research progress in overlap factor correction, layer detection, and signal retrieval for the ground-based Mie lidar to guide future research and application.

Progress The key challenges in Mie scattering lidar data processing include overlap factor correction, layer detection, and signal retrieval (Fig. 1). For overlap factor, the correction methods can be divided into experimental and theoretical methods. The experimental methods do not depend on the lidar system parameters but require the assumption of a uniform atmospheric distribution. The theoretical methods include analytical methods and ray tracing methods, which can guide the design of the lidar system. In addition, the overlap factor effect can be reduced more effectively by adjusting and improving lidar systems, such as dual field-of-view lidar and CCD side-scattering lidar.

For layer detection, the slope-based method can be directly applied to the raw lidar signal but is very sensitive to the noise. The threshold-based method is relatively more robust and commonly used to produce standard products (Fig. 4). However, tenuous layers may be missed because their signal intensity does not consistently exceed the threshold. The hypothesis test method based on the Bernoulli distribution decides whether the signal is a layer or not based on the estimated probability of it belonging to a layer. Studies have shown that its detection performance is superior to the threshold-based methods (Fig. 5).

For signal retrieval, the Fernald method is the most widely used but requires two parameters: the lidar ratio and the boundary value. The boundary value will directly affect the retrieval accuracy (Fig. 6) and can be determined by the fixed scattering ratio method, single-component fitting method, two-component fitting method, and joint observation method. Among them, the two-component fitting method can independently distinguish the contribution of atmospheric molecules, with excellent applicability and high accuracy. Furthermore, an incorrect lidar ratio will cause the overall retrieval deviation (Fig. 7). Methods for determining the lidar ratio mainly include the empirical method, aerosol optical depth (AOD) constraint method, and joint observation method. The popular AOD constraint method can obtain the lidar ratio mean value accurately but lacks its vertical profile distribution. The joint observation method using multiple vertical observations can provide a lidar ratio profile, but there are very few simultaneous vertical observations. In addition, many signal denoising algorithms have also been developed, but it is still a problem to evaluate their performance due to the lack of accurate observations as references.

Conclusions and Prospects Key issues such as overlap factor correction, layer detection, and signal retrieval still exist in ground-based Mie scattering lidar data processing. The development of new technologies such as dual field-of-view lidar and CCD side-scattering lidar provides more possibilities for low-overlap observation. The hypothesis test method can avoid one-size-fits-all empirical judgments and detect layers more accurately than other methods. In the retrieval, accurate boundary value selection requires avoiding simple assumptions and separating aerosol and molecule contributions. In addition, with the development of other vertical observations, the acquisition of lidar ratio profiles has become easier, which largely improves the retrieval accuracy of ground-based Mie scattering lidar.

Key words atmospheric optics; aerosol; overlap factor; layer detection; data retrieval